Numerical Investigation of Low Level OSNR Estimation Based on Gaussian Fitting and NLLS on AAH in Noisy Optical Communication Links

Cristian Castro H.[(1)], Diego H. Peluffo O.[(2)], Oscar Marino Díaz[(3)], Neil Guerrero G.[(4)]
ccastroh89@gmail.com, omdiazb@unal.edu.co, diegohpo@gmail.com, neguego@gmail.com

***Abstract*—An extended digital estimation approach of optical signal to noise ratio (OSNR) based on statistical analysis of asynchronous amplitude histograms (AAH) of the received optical signal is presented and numerically investigated. Accurate OSNR estimation on highly noisy optical transmission link is achieved. Furthermore, the proposed OSNR estimation approach may be digitally adjusted to any Cartesian modulation format such as multilevel phase shift keying and quadrature amplitude modulated optical signals without degrading estimation accuracy. The OSNR estimation methodology is based on kernel density estimation with Gaussian kernels and non-linear least-squares regression (NLLS). Heuristic searches are no longer needed and the process becomes more reliable and robust. Reported results show accurate OSNR estimation with less than 15% error estimation on the simulated OSNR value for different signal modulation formats, exhibiting a more confident estimation system, with comparable results among formats because of the statistical nature histogram instead of the regular counting bins histogram.**

***Index Terms*—Asynchronous amplitude histograms(AAH), gaussian fitting, non-linear least squares(NLLS), optical signal to noise ratio(OSNR), optical performance monitoring systems(OPMS).**

I. Introduction

Next generation broadband hybrid optical transmission systems require accurate monitoring of optical transmission variables such as OSNR and fiber transmission impairments in order to ensure reliable telecommunication services to end users. Moreover, next generation ultra-fast terabit telecommunication systems will require real-time monitoring modules.

Reported optical performance monitoring systems (OPMS) including optical compensation devices have been used to monitor local transmission impairments such as [1]. Nonetheless, monitoring the entire network requires addition of expensive optical devices[2], so this methodology is not advisable; furthermore the hybrid nature of the upcoming optical networks makes necessary an adaptive estimation process and estimation systems must be fast enough and require few data storage for obtaining OSNR estimates before transmission starts given the multiple sources of data in the optical links[3]. Recently demonstrated approaches have pointed out that asynchronous amplitude histograms (AAH), eye diagrams among other statistical analysis of the received optical signal, enhance OPMS by reducing computational cost and improving estimated parameters of the optical transmission [4].

Previous OPMS includes narrow band filters, with tunable parameters for monitoring Wavelength Division Multiplexing (WDM) networks. Even though its performance is acceptable, it has been probed to be a time consuming system[5]. In [6], the assumption of in-band noise equality among center neighborhoods, makes monitoring possible through data interpolation, yet this assumption may not always be true, in some cases such as dense WDM systems, where the channels side-bands are in fact hiding the noise-level among center vicinities[7].

Advantages of AAH for estimating and analyzing optical transmission impairments such as chromatic dispersion, OSNR, and first order polarization mode dispersion (PMD) due to its simplicity and flexibility have been recently shown [8].

We reported in [9], first approach to estimate OSNR for phase shift keying modulated signals, and quadrature amplitude modulated signals (QAM), based on proportional relations between mode variations of histograms and the loaded optical noise to the simulated optical communication link. However, alphabet size was constrained to 2 bits per symbol. The obtained AAH from modulated optical signals with alphabet size equal to $M = 2,4$ for PSK and DPSK systems and $M = 4$ for QAM is a two-mode histogram, this is, histograms are formed by two main peaks with a centered valley. Such peaks are then supposed to be symmetric to the center and constitutes a maximum of the gaussian that compose the modes. However when increasing the alphabet size in QAM, the resulting histogram has more than two modes, so identification of each mode is needed adding complexity to the estimation process.

In this paper we propose an extended approach with a more general estimation system that uses simple pattern recognition and signal processing techniques. In general, the methodology aims to estimate the OSNR of digital modulated signals from an empirical relationship between the mode variation in the AAH and the induced noise. AAH analysis requires mode identification, that is done by means of a gaussian kernel density estimator, since gaussian probability density function (PDF) of the mode is assumed. From such PDF, the OSNR behavior is characterized using the changes in the standard deviation. Empirically we observed an exponential-like shaped curve when plotting standard deviation against OSNR, conse-

quently a non-linear least squares (NLLS) regression is used to estimate the parameters that best fits the exponential-like curve. Gauss-Newton numerical method is applied to solve the resulting non-linear equation system.

Simplicity and fastness of the proposed methodology proved to be reliable in estimating OSNR and low error was obtained maintaining low computational cost requirements for high-speed optical transmission links, additionally simplicity in the proposed scheme makes possible its implementation in low cost devices such as Application Specific Integrated Circuits (ASICs) or Digital Signal Processors.

II. Materials and Methods

The proposed methodology is divided into two main stages. Firstly, a training stage Fig. 1, is made to obtain OSNR estimators for each modulation format, this is done by finding the curve parameters. Secondly, such parameters will be applied for estimating OSNR in randomly generated, non-previously used signals, this corresponds to the testing stage.

Finally to quantify the performance of the estimators, standard errors are calculated.

A. Training

For training each estimator, we must start generating the pseudo-random binary (PRSB) sequences, followed by the transmission through an additive gaussian noise channel. Given the random nature of this process, this can be done as many time and sequence-length as needed.

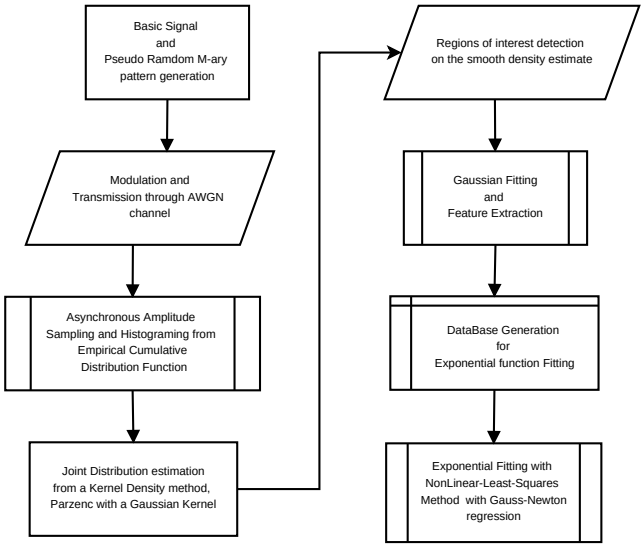

Fig. 1: Diagram of training system.

The length sequence chosen, is made thinking on the application of the propose OPMS in Optical Packet Switched Networks, so as usually transmitted datagrams in packet switching networks consist in 1500 bytes we produce a PRSB of 12000 bits, and modulate in each of the mentioned formats with a sinusoid shaping for the upcoming sampling.

So, as each symbols is shaped into a sinusoid signal, we randomly sample this sinusoid with a mediocre sampler, so few data storage is needed. Where in Fig. 2 we have usually that $\tau_1 \neq \tau_2 \neq \ldots \neq \tau_n$ and the number of samples per symbol is between 8 and 16, which is a low sampling taking into account that no clock is used for obtaining the histogram.

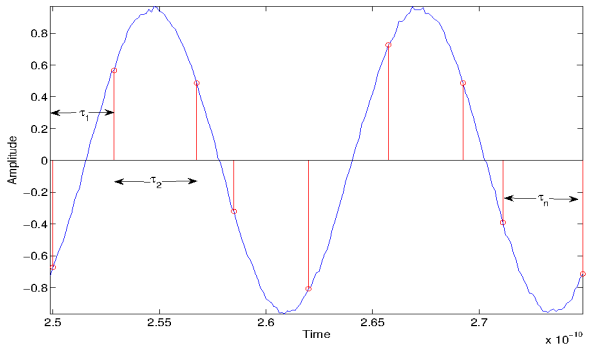

Fig. 2: Randomly sampling of sinusoid signal.

Next we obtain the asynchronous amplitude histogram, the histogram is now calculated not directly from the occurrences of an amplitude in a given bin, but with the empirical cumulative distribution function (ECDF), this allow us to maintain the amplitude range of the original signal instead of scaling it to the bins number. This is done to maintain a certain concept of comparability among every estimator in the different modulations formats. While the regular histogram Fig. 3(a) gives bins counts represented by each bar height, ECDF provides an histograms area normalized which bar heights are computed from the increases in the ECDF Fig. 3(b).

After the histogram is generated, is necessary to separate or identify its modes, for this we used a kernel density estimation, more exactly a Parzen estimator [10] with a gaussian kernel for obtain the joint distribution estimation of the complete histogram, this gives us a smooth curve over the histogram with no spurious peaks if the kernel width is chosen correctly.

Fig. 4 shows the resulting density estimation for multimodal histograms with a Parzen density estimation, red line, and the peaks and valleys detection (purple and green lines respectively).

Parzen density estimation is done by fixing the bins volume among the space and adding each contribution. Such contribution is defined by the ”bin-shape”, i.e. the probability function kernel K placed at each bin position, which must satisfy

$$K(\cdot) : \left\{ K(r) > 0, \quad \int K(r)\,dr = 1 \right\}$$

Considering the gaussian-like envelope of the mode histograms, the chosen kernel was a gaussian function, resulting in the following Parzen density estimator for test objects x

$$p(z) = \frac{1}{hn} \sum_i K\left(\frac{z - x_i}{h}\right) \quad (1) \qquad K(x) = \frac{1}{h\sqrt{2\pi}} e^{\left(\frac{x^2}{2h^2}\right)} \quad (2)$$

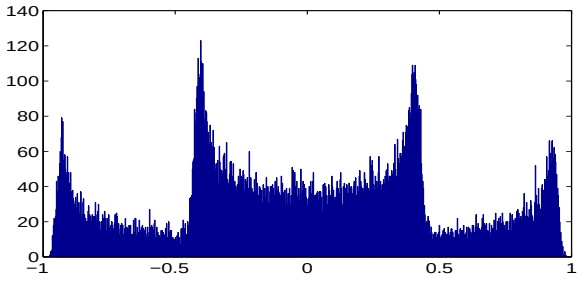

(a)

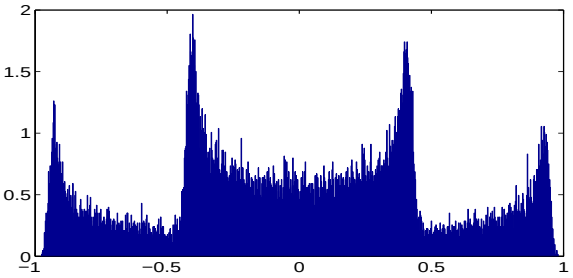

(b)

Fig. 3: Different histograms of a randomly sampled 8−QAM signal: 3(a) Regular histogram. 3(b) Histogram of the empirical cumulative distribution function of the sampled data.

Free parameter h, determines the width of each gaussian to be placed, this will controlled how well the obtained curve will fit the histogram, however since we assume mode independence given the random sampling, we just used the density estimator for obtaining the regions of interest to each mode.

After smoothing the distribution function, the mode separation is done by detecting local minima and maxima in the joint distribution curve, this gives us a confidence region for estimating the parameters of the Gaussian function that best fits each modes. Fig. 5(a) shows an standard normal distribution function, with mean μ and standard deviation σ; as seen, the mean parameter of the function is horizontally located at the maximum of the function, this is

$$\underset{i=1\ldots n}{\mu_i} = \max_z \{p(z)\}$$

where $p(z)$ is the joint distribution obtained with the Parzen estimator 1 and n is the number of modes observed in it.

Given the normal PDF function

$$N(\mu,\sigma) = \frac{1}{\sqrt{2\pi}\sigma} e^{-\left(\frac{x-\mu}{\sigma}\right)^2}$$

which that is maximum when $x = \mu$, we have that

$$\sigma = \frac{1}{\sqrt{2\pi}\max(\hat{\mathbf{n}})}$$

where $\hat{\mathbf{n}}$ is the normalized section of the histogram to which the mode belongs, this must be done, since the obtained

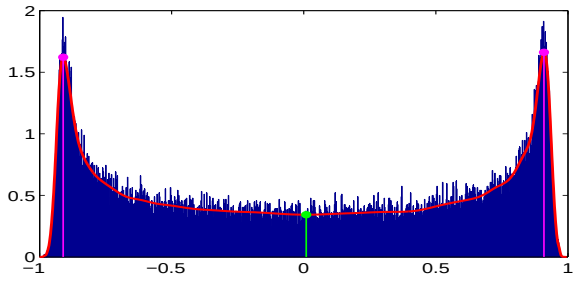

(a)

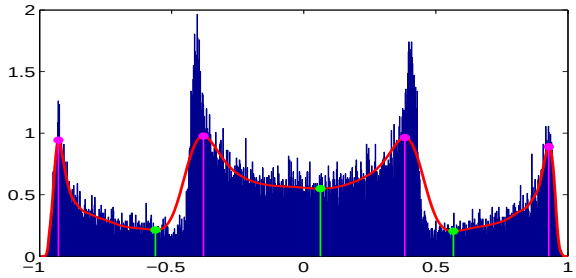

(b)

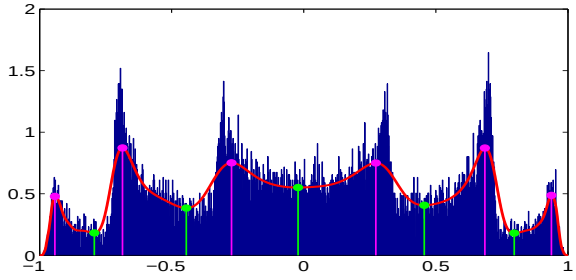

(c)

Fig. 4: Parzen Estimation and Region of interest detection: 4(a) $M-$PSK, $M-$DPSK and 4−QAM signals. 4(b) 8−QAM signal. 4(c) 16−QAM signal.

histograms comes from the ECDF of the data, then re-scaling the data for individual estimation is necessary.

Fig. 5(b) shows the resulting fitting approximations given the found parameters, each mode then provides us with two features for the OSNR contained in the sampled signal. Fig. 6(a) and Fig. 6(a) are the corresponding results for $8,16$-QAM signals. Each parameter vector, (mean and standard deviation), will then constitute features for the OSNR of the signal at hand.

The relationship found between the behavior of the standard deviation of the Gaussian function fitting each mode and the OSNR in the signal, showed an exponential-like curve, Fig. 7, blue stem dots; then a NLLS algorithm with a Gauss-Newton regression is used for finding the exponential parameters [11],[12].

The NLLS problem is an unconstrained minimization problem of the form

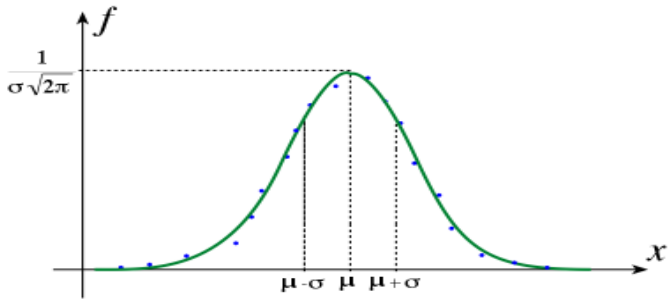

(a)

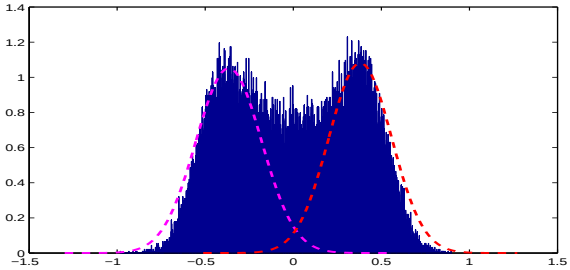

(b)

Fig. 5: 5(a) Normal Distribution Function, mean μ and standard deviation σ. 5(b) Histogram and gaussian fits for a 4−QAM signal.

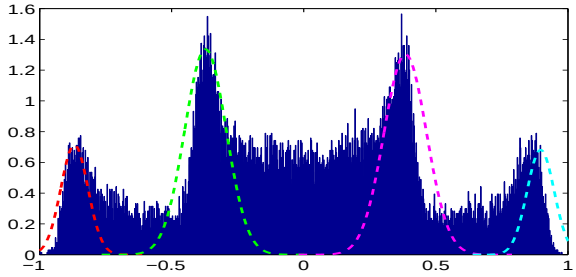

(a)

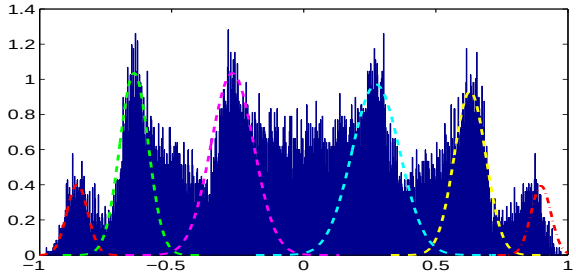

(b)

Fig. 6: Histograms and Gaussian Fits for: 6(a) 8−QAM signal, 6(b) 16−QAM signal.

$$\min_x f(x) = \sum_{k=1}^{m} f_k(x)^2 \quad \text{with} \quad f(x) = Ae^{(Bx)} \tag{3}$$

Then the minimization problem becomes finding the minimum of

$$E(A,B) = \sum_{k=1}^{m} \left(Ae^{(Bx_k)} - y_k\right)^2 \tag{4}$$

The partial derivatives of 4 within respect A and B respectively are

$$\frac{\partial E}{\partial A} = 2\sum_{k=1}^{m} \left(Ae^{(Bx_k)} - y_k\right)\left(e^{(Bx_k)}\right) \tag{5}$$

$$\frac{\partial E}{\partial B} = 2\sum_{k=1}^{m} \left(Ae^{(Bx_k)} - y_k\right)\left(Ax_k e^{(Bx_k)}\right) \tag{6}$$

For solving this minimization problem we must equal 5 and 6 to zero and simplify for solving this is

$$A\sum_{k=1}^{m} e^{(Bx_k)} - \sum_{k=1}^{m} y_k e^{(Bx_k)} = 0 \tag{7}$$

$$A\sum_{k=1}^{m} x_k e^{(2Bx_k)} - \sum_{k=1}^{m} x_k y_k e^{(Bx_k)} = 0 \tag{8}$$

However, this is a consuming task depending of the number of observations, so numerical methods as Gauss-Newton are used.

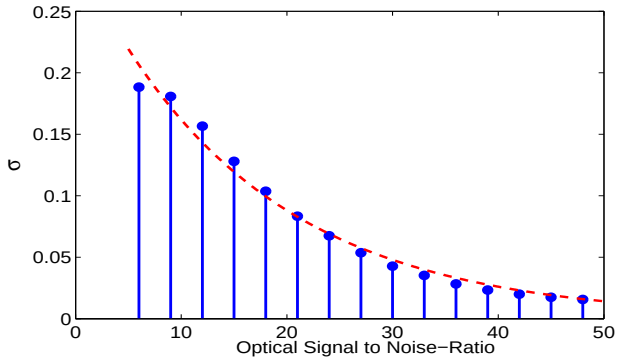

Fig. 7: Exponential curve (red) overlapped with the σ vector(blue) for a 4−QAM signal, parameters $A = 0.2973$, $B = -6.0826E-2$.

In Fig. 7 we can see an exponential curve (dashed red line) function estimated via NLLS for a 4−QAM signal. Found parameters were $A = 0.2973$ and $B = -6.082E-2$. So the exponential function is

$$\sigma = 0.2973e^{-6.082E^{-2}x_{OSNR}}$$

B. Testing

Testing was done by measuring the standard error of the estimated OSNR with the real noise added to the signal. Hence the stages for testing the estimator are the same from the beginning to the feature extraction of the normal distributions, after this inverse exponential function, this is solving 3 for x, where x represents the OSNR, then

$$x_{OSNR} = \frac{\ln(\sigma) - \ln(A)}{B} \tag{9}$$

and the standard error function

$$E_{std} = \frac{1}{N}\sum_{i=1}^{N}\left|\frac{x_i^t - x_i^p}{x_i^t}\right|$$

with x_i^t and x_i^p being the theoretical (real) and practical (found) OSNR of each signal tested.

III. Experimental Setup

Diversity and reproductivity of the estimators was achieved by generating 25 sequences for each of the 15 ($M-$PSK and $4-$QAM) and 12 ($8-$QAM and $16-$QAM) noise levels used for the modulation formats. Lowest limit for the first cases was set in $6dB$ and 15 since below this value, mode differentiation in the obtained histograms was lost, this can be seen in Fig. 8.

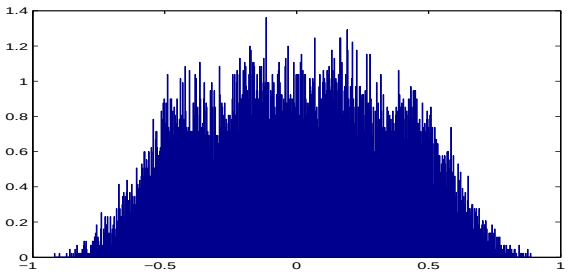

Fig. 8: Histogram with low OSNR value for a $16-$QAM signal with $OSNR = 12dB$

Now, each of the 25 sequences, both in the training and testing process, passed through the feature extraction process, this is smoothing the histogram with a low-pass filter, in this case, we used a moving averaged filter with a 5 step window. The Parzen estimator for the joint PDF, was set with a kernel window $h = 0.125$ that seemed to work well enough for any case.

After feature extraction is made, standard deviation matrixes are formed so results are easily managed in the form

$$\boldsymbol{\Sigma}^p = \begin{bmatrix} \sigma_{11} & \cdots & \sigma_{1n} \\ \vdots & \ddots & \vdots \\ \sigma_{m1} & \cdots & \sigma_{mn} \end{bmatrix}$$

where $m = 1...15(12)$ manage the OSNR levels, $n = 1...(2)(4)(6)$ is the numbers of modes found in each modulation format and $p = 1...25$ are the iteration sequence. Then summarization of results is made as follows

First, exponential is fitting via NLLS is applied to each σ row-wise, and matrix parameters are formed

$$\boldsymbol{A} = \begin{bmatrix} A_{11} & \cdots & A_{1n} \\ \vdots & \ddots & \vdots \\ A_{p1} & \cdots & A_{pn} \end{bmatrix} \quad \boldsymbol{B} = \begin{bmatrix} B_{11} & \cdots & B_{1n} \\ \vdots & \ddots & \vdots \\ B_{p1} & \cdots & B_{pn} \end{bmatrix}$$

And summarized exponential parameters are created as

$$\bar{A_n} = \frac{1}{p}\sum_{k=1}^{p} A_{pn} \quad \alpha_n = std\left(\boldsymbol{A}_n = \begin{bmatrix} A_{1n} & \cdots & A_{pn} \end{bmatrix}\right)$$

$$\bar{B_n} = \frac{1}{p}\sum_{k=1}^{p} B_{pn} \quad \beta_n = std\left(\boldsymbol{B}_n = \begin{bmatrix} B_{1n} & \cdots & B_{pn} \end{bmatrix}\right)$$

With α and β being the standard deviations of the exponential curve parameters.

IV. Results and Discussion

Robustness of the NLLS algorithm make the estimators strongly reliable, and reproductivity of the estimators can be prove by comparing individual curve-parameters for a single pattern in a determined modulation format with the general averaged parameters expecting low errors.

Table I show the summary of the found parameters for each of the modulation formats, experiments revealed that the symmetry in the histograms provided with almost equal values of σ and center opposite values of μ for the gaussian fits in the corresponding modes; this is, each mode has an associated amplitude, either positive or negative, the values of σ are the same for the negative mode associated to its positive, then summarization is made also averaging the modes values.

TABLE I: Parameters Summary with Individual Methodology

Format	A	α	B	β
$2-$DPSK	0,3014353	0,00556475	-0,060811	0,00086144
$4-$DPSK	0,2950926	0,00872765	-0,0605182	0,00130382
$2-$PSK	0,3009671	0,00700565	-0,0607758	0,00110682
$4-$PSK	0,2960797	0,00999807	-0,0605827	0,00139807
$4-$QAM	0,2952689	0,00815366	-0,0605679	0,00111414
$8-$QAM	0,2884273	0,02467880	-0,0742489	0,00306138
	0,2233583	0,01172513	-0,0387567	0,00186877
$16-$QAM	0,1913273	0,02843192	-0,0695270	0,00457866
	0,1811065	0,01199731	-0,0491510	0,00222466
	0,1944609	0,00895000	-0,0317187	0,00157991

Errors presented were usually under the 10%, showing an acceptable estimation, moreover this error percentage can be attributed and corrected by the standard deviations of the parameters in the exponential curves. Even for $8-$QAM and $16-$QAM errors were low, showing an improve of the methodology with a low increase in complexity and computational cost. In Table II is the summarized error percentage for all seven modulation formats, as seen results are under 10%. Where μ_{err} and σerr stand for the mean and standard deviation of the error. Figures 9-12 present the error performance for all 25 iterations in some of the modulation formats tested.

TABLE II: Error Summary for Individual Methodology

Format	μ_{Err} (%)	σ_{Err}
2−PSK	6,50253752	1,56425153
2−DPSK	6,19198634	1,49379924
4−PSK	6,3575341	1,84405445
4−DPSK	6,46195194	1,8422269
4−QAM	6,1101992	1,93074169
8−QAM	6,49772816	1,44549586
16−QAM	5,47506134	1,41950518

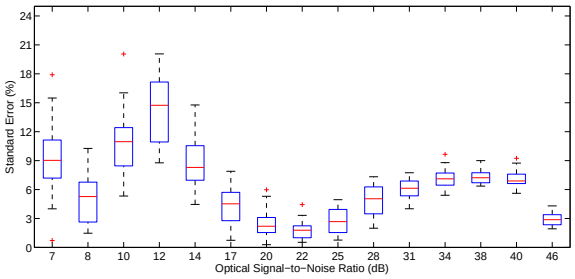

Fig. 9: Error performance of Estimation in 4−PSK signals.

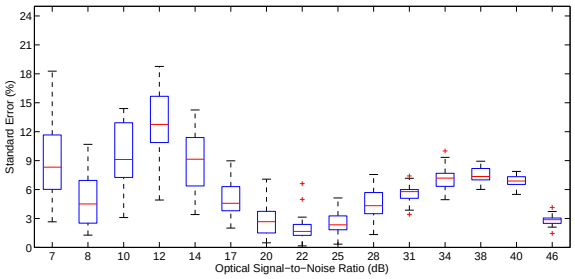

Fig. 10: Error performance of Estimation in 4−QAM signals.

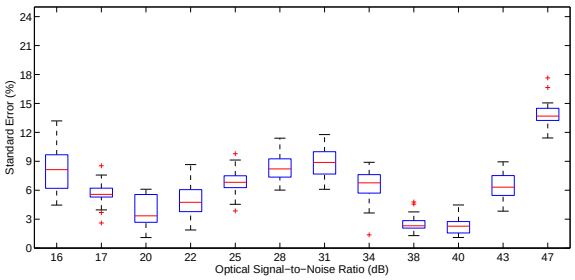

Fig. 11: Error performance of Estimation in 8−QAM signals.

V. Conclusions and Future Work

It is possible to estimate the OSNR without knowing its real nature or causes. Moreover no clock signal is needed because of the randomness of the sampling. The novel use of an statistical approach gives us the possibility of compare how well the estimation is carried out in distinct modulation formats since no amplitude constraint exists and only probabilistic information is used.

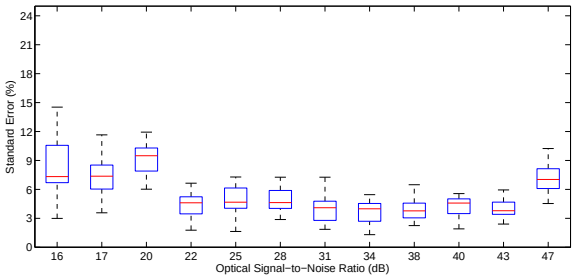

Fig. 12: Error performance of Estimation in 16−QAM signals.

Enhancement of the previously proposed methodology [9] was successfully performed with little complexity addition, and moreover the estimator was extend for higher modulation formats with acceptable results.

In addition all heuristically processes were eliminated and all algorithms and mechanism used are mathematically grounded hence the coherence and robustness of the estimators stand as one of its most important characteristics. Finally the proposed OPMS based on AAH, can be enhanced using histogram based coefficient as features and observing their behavior with respect to the changes in the OSNR.

References

[1] C. Weinert, "Gaussian deconvolution method for identification of impairments in optical signal transmission," *J. Opt. Netw.*, vol. 3, no. 6, pp. 381–387, Jun 2004.

[2] C. C. K. Chan, *Optical Performance Monitoring: Advanced Techniques for Next-Generation Photonic Networks*. Elsevier Inc., 2010.

[3] S. Sarkar, S. Dixit, and B. Mukherjee, "Hybrid wireless-optical broadband-access network (woban): A review of relevant challenges," *Lightwave Technology, Journal of*, vol. 25, no. 11, pp. 3329 –3340, nov. 2007.

[4] R. Luis, A. Teixeira, and P. Monteiro, "Optical signal-to-noise ratio estimation using reference asynchronous histograms," *Lightwave Technology, Journal of*, vol. 27, no. 6, pp. 731 –743, march15, 2009.

[5] X. Lin and L. Yan, "Multiple-channel osnr monitoring with a single detector," *Photonics Technology Letters, IEEE*, vol. 16, no. 12, pp. 2637 –2639, dec. 2004.

[6] M. Petersen and T. Tokle, "Novel osnr monitoring technique in dense wdm systems using inherently generated cw monitoring channels," in *Optical Fiber Communication and the National Fiber Optic Engineers Conference, 2007. OFC/NFOEC 2007. Conference on*, march 2007, pp. 1 –3.

[7] M. Skold, B.-E. Olsson, H. Sunnerud, and M. Karlsson, "Pmd-insensitive dop-based osnr monitoring by spectral sop measurements," in *Optical Fiber Communication Conference, 2005. Technical Digest. OFC/NFOEC*, vol. 4, march 2005, p. 3 pp. Vol. 4.

[8] I. Shake and H. Takara, "Chromatic dispersion dependence of asynchronous amplitude histogram evaluation of nrz signal," *Lightwave Technology, Journal of*, vol. 21, no. 10, pp. 2154 – 2161, oct. 2003.

[9] J. M. Lǿpez, D. H. Peluffo-Ordoñez, O. M. Díaz, and N. Guerrero, "Low level optical signal to noise ratio measurement using basic statistical data from asynchronous amplitude histogram gaussian fitting," in *IBERCHIP XVII, 2011*, 2011.

[10] E. Parzen, "On estimation of a probability density function and mode," *The Annals of Mathematical Statistics*, no. 3, pp. pp. 1065–1076.

[11] A. Bjork, *Numerical Methods for Least Squares Problems*. Society for Industrial and Applied Mathematics., 1996.

[12] K. P. Chong and S. H. Zak, *An Introduction to Optimization*, 2nd ed. Jonh Wiley and Sons, Inc., 2001.